Rare Metal Materials and Engineering
Volume 50, Issue 3, March 2021
Available online at www.rmme.ac.cn

Science Press

Cite this article as: Rare Metal Materials and Engineering, 2021, 50(3): 0848-0852.

ARTICLE

High Mobility Ti-doped In_2O_3 Films Used for Amorphous/Crystalline Silicon Heterojunction Solar Cells

Huang Jin[1], Bao Shaojuan[1], Lu Linfeng[2], Yang Ji[1], Bai Yanhui[1], Zhang Juan[1], Gao Yong[1], Wang Jilei[1]

[1] HJT Solar Cell Project R & D, Jinneng Clean Energy Technology Ltd, Jinzhong 030300, China; [2] Thin Film Optoelectronic Technology Center, Shanghai Advanced Research Institute, Chinese Academy of Sciences, Shanghai 201210, China

Abstract: A newly Ti-doped In_2O_3 rotary target was used to prepare transparent conductive oxide (TCO) films for amorphous/crystalline silicon heterojunction solar cells. The changes in electrical and optical properties of TCO films were investigated based on T100 thin films deposited with various O_2 contents and compared with indium tin oxide (ITO). Results show that a columnar structure is observed and exhibits high quality of optical performance. Maximum mobility of 75.6 $cm^2 \cdot (V \cdot s)^{-1}$ is observed in Ti-doped In_2O_3 films. Compared to the results of ITO films, it is verified that the cell conversion efficiency based on the heterojunction (HJT) production line improves by 0.26% of T100 material, mainly benefiting from the excellent electrical transport properties, as well as the high transparency.

Keywords: Ti-doped In_2O_3; transparent conductive oxide (TCO) film; heterojunction solar cell

Silicon heterojunction (HJT) solar cells exhibit very high efficiencies with excellent surface passivation of hydrogenated amorphous silicon (a-Si:H) films[1-3]. During the process, transparent conductive oxide (TCO) layers are deposited on the front and rear sides of the HJT solar cell. These TCO layers facilitate carrier conductance for efficient current collection and transfer the collected current to electrode terminals. Meanwhile, the front TCO layers are expected to serve as antireflection coatings in HJT configuration[4-9]. Many efforts were made in recent years to better combine excellent optical properties with electrical properties. It is recognized as the key issue to gain proper ohmic contact between TCO material and doped p and n-type a-Si:H layers for the improvement of cell performance[10-15], especially in short current (I_{sc}) and fill factor (FF) of the HJT solar cells.

Among series of commercially TCO materials, -W/-Sn-doped In_2O_3 has been widely used on PV devices, due to its high electrical conductivity and high transmission in the visible spectral. Van et al[16] prepared titanium-doped indium oxide by sputtering and observed a maximum mobility of 83.3 $cm^2 \cdot (V \cdot s)^{-1}$. Gupta et al[17] studied titanium-doped indium oxide using the technique of pulsed laser deposition (PLD) and obtained the mobility of 159 $cm^2 \cdot V^{-1}$ grown at 600 °C, which is the highest mobility ever of doped In_2O_3 films. This apparent enhancement in electrical feature suggests that the titanium-doped indium oxide has large potential application in PV. However, few works about using Ti-doped In_3O_2 on HJT solar cells were reported.

In this research, various Ti-doped In_2O_3 (T100) thin films were fabricated with different O_2 contents under the Ar atmosphere. The crystallization, resistivity and transmittance of T100 films were investigated. The optical and structural property differences between T100 and typical indium tin oxide (ITO) were systematically investigated. The T100 films were optimized to obtain better performance based on HJT devices, as well as on the mass production of HJT solar cells.

1 Experiment

Received date: March 09, 2020
Corresponding author: Huang Jin, Master, HJT Solar Cell Project R & D, Jinneng Clean Energy Technology Ltd, Jinzhong 030300, P. R. China, E-mail: 466478431@qq.com

All solar cells in this work were fabricated through the same process using n-type Si substrates of M2 size (156.75×156.75 mm^2) with a resistivity of 5 Ω·cm. At first, wafers were executed by saw. Then, etched wafers with both sides were achieved. Texturing treatment of substrates was carried out, and then the wafers were cleaned in SC1 and SC2. The perfect wafer surface was achieved with a final thickness of 160 μm and pyramids size of 5 μm. Doped and intrinsic hydrogenated amorphous silicon (a-Si:H) layers were deposited on both sides, with a n-type/intrinsic stack (n/i) on the front side and a (p/i) stack on the rear, corresponding to the "rear-emitter" HJT architecture[18]. Then, TCO layers were deposited on both sides by DC magnetron sputtering from rotatory targets under Ar/O_2 gas mixtures atmosphere. It should be mentioned that the rear TCO of each group was made of ITO material. The front TCO films were prepared by ITO and T100 targets respectively. ITO layers were sputtered from a rotatable target of In_2O_3:SnO_2= 90:10. Metal grids were screen-printed with a silver paste, using a 5-busbar pattern. Finally, the cells were annealed at 200 °C for 30 min in order to cure the silver paste. Film thickness was measured using 4-probes measurement.

To characterize the properties of ITO and T100 films, these films were deposited on SiO_2-coated soda-lime-silicate glass substrates at room temperature. Considering the drying and sintering effect of post-annealing on the structure in fabricating a-Si/C-Si heterojunction solar cells, the electrical and optical properties of the T100 films were annealed at about 200 °C before all the characterization tests. Sheet resistance was measured by the four-point probe method, and the Hall effect measurement was performed by Van der Pauw method to evaluate the carrier density and Hall mobility of thin films. The thickness of thin films was measured by SE 800PV ellipsometer. X-ray diffraction (XRD, using Cu Kα radiation) measurement was carried out to evaluate the crystal structure of thin films. Optical measurement was performed to estimate the transmittance of TCO thin films. ITO films were deposited with the best conditions as references.

2 Results and Discussion

2.1 Microstructure of as-received coating

Fig.1 describes XRD patterns of post-annealed ITO and T100 thin films deposited with different oxygen flows at the substrate temperature of 90 °C. ITO shows extremely weak diffraction peak at 2θ=30.7°, which is preferentially indexed to the cubic bixbyite-type In_2O_3 polycrystalline structure[19-21]. Interestingly, it is observed that all of the T100 films have the strong diffraction peak at 2θ=30.7° and weak diffraction peaks at 2θ=21.4°, 35.5°, 61.4°, 51.0°, indicating that the T100 films are better crystallized after the annealing process. It can be attributed to the facility of Ti^{4+} in grain growth. The ionic radius of Ti^{4+} (0.068 nm) is smaller than that of In^{3+} (0.092 nm) or Sn^{4+} (0.071 nm), leading to strong crystalline growth in T100 films. According to the results summarized in Fig.1, the T100 films has typical polycrystalline structures with the weak diffraction peaks of (122), (400), (431), (440) and (622), and main diffraction peak of (222) when the oxygen flow increases from 3 mL/min to 6 mL/min. Furthermore, the diffraction intensity of (222) peak increases implying that the improvement of crystalline grain corresponds with the increase of oxygen flow.

Fig.2a~2d show T100 film morphologies of surface and cross-section with the increase of O_2 flow from 3 mL/min to 6 mL/min, Fig.2e illustrates the morphologies of ITO film. According to the measuring scale, both T100 and ITO films have nanocrystalline property. Compared to T100 profiles, ITO film shows a smoother cross section and smaller crystalline grain size, corresponding to the results of XRD analysis. On the contrary, T100 films exhibit disorganized structure, and the cross-sectional structure of T100 changes markedly with the increase of O_2 flows. A columnar structure perpendicular to the substrate is visible when O_2 flow is 6 mL/min, which is prone to enhance the visible light transmittance[22,23].

2.2 Optical and electrical properties

The electrical properties of the T100 and ITO films are analyzed by Hall-effect measurement. Fig.3 illustrates the carrier concentration (n) and mobility (μ) of the annealed films as a function of O_2 flow. A general tendency of increase at first and decrease afterwards is observed in the Hall mobility with increasing the O_2 flow. T100 film gets the highest value of 75.6 $cm\cdot(V\cdot s)^{-1}$ when the O_2 flow is 4 mL/min. It is clear that the values of carrier concentration of T100 films are very sensitive to the oxygen flow. Different from the tendency of Hall mobility, the carrier concentration shows a downtrend from 2.0×10^{20} cm^{-3} to 1.16×10^{20} cm^{-3}. The oxygen vacancies are gradually filled by inducing excess oxygen, leading to the reduction of carrier concentration. As shown in Fig.4, the resistivity of these films is sensitive to the oxygen content during deposition. On basis of the optical and electrical analysis, the key to combine high conductivity with optical transmission for better films is optimizing the O_2/Ar component.

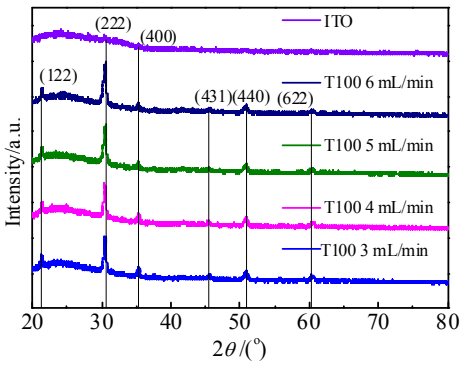

Fig.1 XRD patterns of ITO and T100 films with different O_2 flows

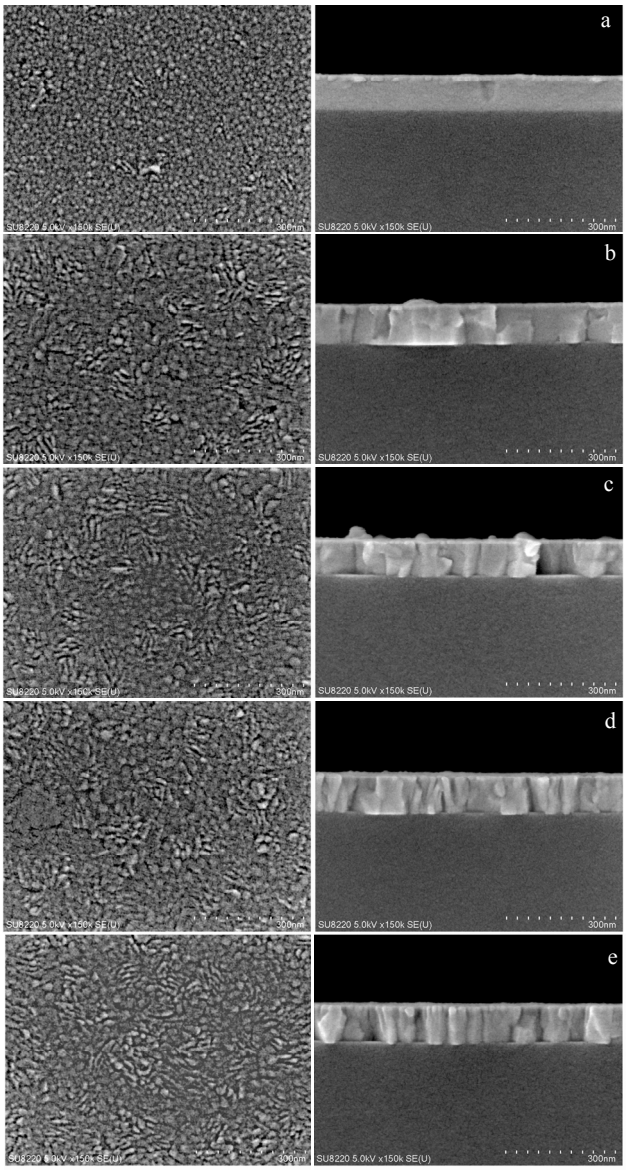

Fig.2 SEM morphologies of surface and cross-section of T100 films with different O_2 flows (a~d) and ITO film (e): (a) 3 mL/min, (b) 4 mL/min, (c) 5 mL/min, and (d) 6 mL/min

Fig.4 illustrates the optical features in the UV-visible-NIR region (from 300 nm to 850 nm) of the ITO and T100 films grown on glass under various O_2 flows. All of the T100 films fabricated under different oxygen flows exhibit higher transmittance than ITO in the visible region. The higher transmittance of T100 films might be explained by the lower carrier concentration of T100 films than that of ITO sample (Fig.3), decreasing optical absorption by excess free carries density. In the aspect of T100 series, both the transmittance and reflectance peaks shift toward the red region with the increase of the oxygen content. It is known that the bandgap of indium tin oxygen compound films increases with the increase of carrier concentration by the Burstein-Moss (BM) effect. The redshift of T100 films might also be explained by the lower carrier concentration with the increase of O_2 flow from 3 to 6 mL/min by BM effect.

T100 and ITO with the thickness of 100 nm were applied on the HJT solar cell as the transparency electrodes. HJT solar cells in this research were fabricated through regular processes, and then formed as the final configuration in Fig.5. In this structure of HJT solar cell, the commercial n-type Cz-Si wafer was used as the absorber layer. The intrinsic a-Si:H layers can passivate the dangling bonds on the surfaces of Si wafer in order to suppress the carrier recombination. The p/n a-Si:H layers with n-type wafer can construct the in-built electrical field and back surface field (BSF) of solar cell. And the TCO deposition process on the a-Si/C-Si stack plays the critical role for short-circuit current J_{sc} and FF of solar cell[24,25]. Based on the rear-emitter design, regular ITO with 10wt% SnO_2 was sputtered as back TCO electrode. The n-side TCO materials studied in this research is deposited by T100, referring to ITO. O_2 flow to ITO varies keeping the total stack thickness constant.

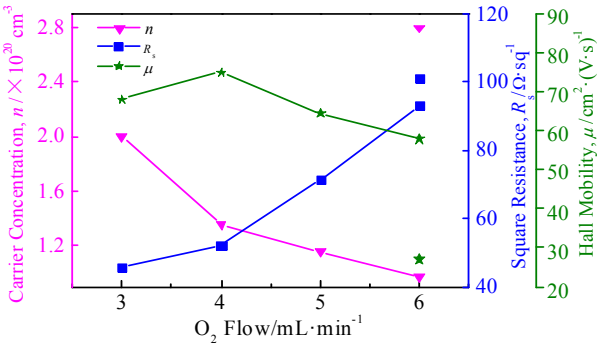

Fig.3 Carrier concentration, square resistance and Hall mobility of T100 films with different O_2 flows (the parameters of ITO are described as the isolated data points)

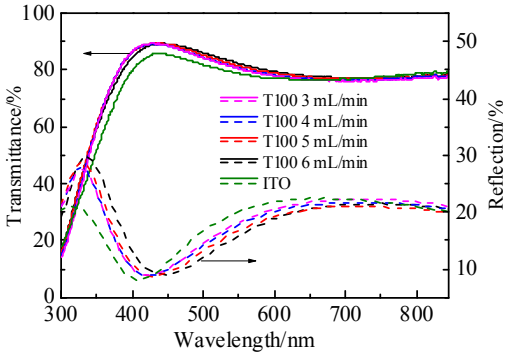

Fig.4 Optical transmittance/reflectance spectra of ITO and T100 films with various O_2 flows

Fig.6 shows cell performances using sputtered ITO and T100. In the aspect of T100 groups, J_{sc} shows rapid increase with increasing the O_2 flow. This improvement is caused by the improvement of optical response (Fig.4), further ascribed to less free carrier absorption. Simultaneously, high quality T100 can improve photon absorption and carrier collection. FF displays progressive reduction with increasing the O_2 flow from 3 mL/min to 6 mL/min. Besides, FF of T100 cell is lower than that of ITO reference, owing to the mismatch between T100 and adjacent contact layers. The relationship between J_{sc} and fill factor of solar cells is similar to the "seesaw effect"[18,26]. The behavior of conversion efficiency is a comprehensive manifestation of J_{sc} as well as FF for HJT cell. Replacing front TCO from ITO to T100, significant improvement of external quantum efficiency (EQE) is observed in Fig.7. The enhancement within 500~900 nm can be attributed to the high transparency of T100. The improvement within 900~1100 nm can be accounted for the better transmittance and lower carrier concentration. Finally, T100 material gets its best efficiency when the O_2 flow is 4 mL/min, increasing by 0.26% (abs.) of the terminal cell efficiency in mass production.

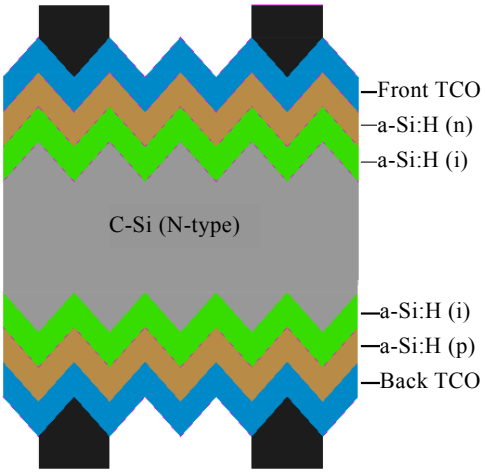

Fig.5 Bifacial configuration of HJT solar cell

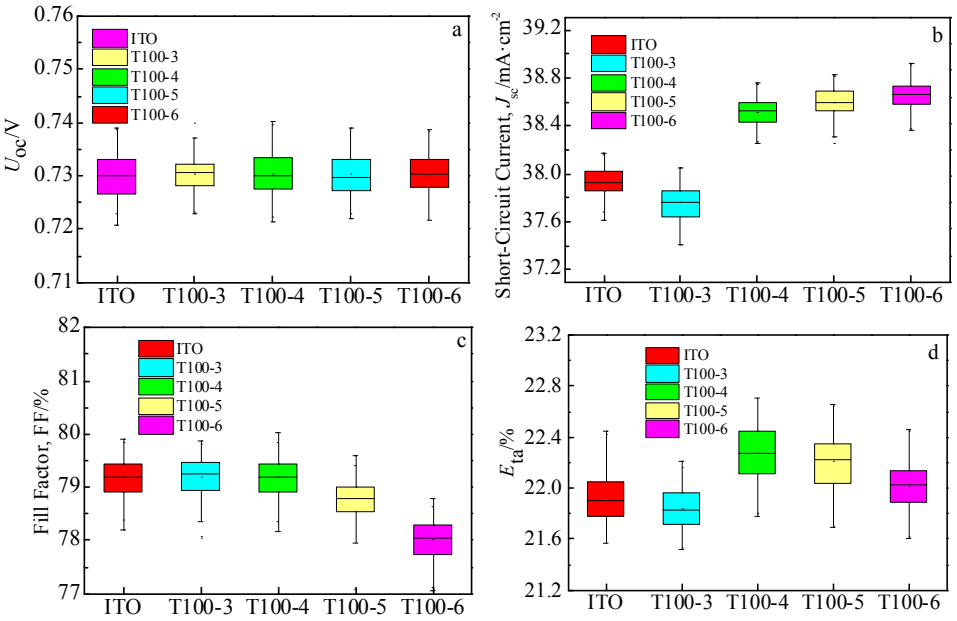

Fig.6 Efficiency parameters U_{oc} (a), J_{sc} (b), FF (c), and E_{ta} (d) of ITO and T100 groups solar cells with different O_2 flows

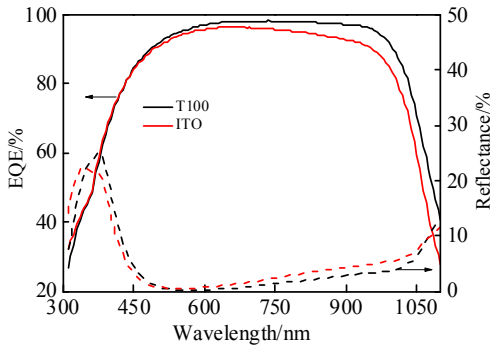

Fig.7 External quantum efficiency (EQE) plots of T100 and ITO solar cells

Fig.7 shows the external quantum efficiency (EQE) spectra for T100 (under the condition of setting O_2 flow as 4 mL/min) and ITO solar cells. The EQE of T100, which increases in a wide range of wavelengths between 300 and 1100 nm, apparently increases in the short wavelength range (600~1100 nm) because of the slight carrier parasite absorption. A discrepancy between T100 and ITO cells is observed at the range of short wavelength (300~400 nm) which can be explained by the Burstein-Moss (BM) effect, indicating the redshift of T100 induced by the lower carrier concentration. These results indicate that the T100 material enables light to reach the silicon wafer with higher effi-

ciently. Especially, the short-circuit current (J_{sc}) of T100 significantly increases to 0.57 mA·cm^{-2}.

3 Conclusions

1) T100 thin films with various O_2 contents and ITO reference can be prepared on glass substrates by DC sputtering.

2) T100 shows relatively poor optical properties in transmittance and high carrier concentration. A columnar structure perpendicular to the substrate is observed based on T100 films, exhibiting relatively high quality on optical performance.

3) The T100 films possess high conductivity and excellent transparency, which contribute to prominent improvement of short-circuit current J_{sc} on heterojunction solar cells, leading to an absolute efficiency gain of 0.26% in mass production.

4) The superior material properties show potential applications for heterojunction technology.

References

1 Adachi D, Hernandez D J, Yamamoto K. *Applied Physics Letters*[J], 2015, 107: 233 506

2 Green M A, Hishikawa Y, Warta W *et al. Progress in Photovoltaics: Research and Applications*[J], 2017, 25: 668

3 Bullock J, Hettick M, Geissbühler J *et al. Nature Energy*[J], 2016(1): 15031

4 Kerkache L, Layadi A, Dogheche E *et al. Journal of Physics D: Applied Physics*[J], 2006, 39: 184

5 Calnan S, Tiwari A N. *Thin Solid Films*[J], 2010, 518: 1839

6 Meng Fanying, Shi Jianhua, Shen Leilei *et al. Japanese Journal of Applied Physics*[J], 2017, 56: 04CS09

7 Grew B, Bowers J W, Lisco F *et al. Energy Procedia*[J], 2014, 60: 148

8 Erfurt D, Heinemann M D, Körner S *et al. Materials Science in Semiconductor Processing*[J], 2019, 89: 170

9 Meng Fanying, Shi Jianhua, Liu Zhengxin *et al. Solar Energy Materials and Solar Cells*[J], 2014, 122: 70

10 Rached D, Mostefaoui R. *Thin Solid Films*[J], 2008, 516: 5087

11 Hussain S Q, Oh W K, Ahn S H *et al. Vacuum*[J], 2014, 101: 18

12 Wolf S D, Descoeudres A, Holman Z C *et al. Green*[J], 2012, 2: 7

13 Bruhat E, Desrues T, Grange B *et al. Energy Procedia*[J], 2017, 124: 829

14 Ritzau K U, Bivour M, Schröer S *et al. Solar Energy Materials and Solar Cells*[J], 2014, 131: 9

15 Lee S Y, Choi H, Li H *et al. Solar Energy Materials and Solar Cells*[J], 2014, 120: 412

16 Van Hest M F A M, Dabney M S, Perkins J D *et al. Applied Physics Letters*[J], 2005, 87: 032 111

17 Gupta R K, Ghosh K, Mishra S R *et al. Materials Letters*[J], 2008, 62: 1033

18 Sai H, Oku Ti, Sato Y *et al. Progress in Photovoltaics: Research and Applications*[J], 2019, 27: 1061

19 Steinhauser J, Faÿ S, Oliveira N *et al. Applied Physics Letters*[J], 2007, 90: 142 107

20 Koida T, Fujiwara H, Kondo M *et al. Journal of Non-Crystalline Solids*[J], 2008, 354: 2805

21 Wardenga H F, Frischbier M V, Morales-Masis M *et al. Materials*[J], 2015, 8: 561

22 Parida B, Gil Y, Kim H *et al. Journal of Nanoscience and Nanotechnology*[J], 2019, 19: 1455

23 Ling Dong, Zhu Guisheng, Xu Huarui *et al. Materials*[J], 2019, 12: 958

24 Hussain S Q, Kim S, Ahn S *et al. Solar Energy Materials and Solar Cells*[J], 2014, 122: 130

25 Ulyashin A, Sytchkova A. *Physica Status Solidi (a)*[J], 2013, 210: 711

26 Yu Cao, Yang Miao, Dong Gangqiang *et al. Japanese Journal of Applied Physics*[J], 2018, 57: 08RB15

高迁移率的钛掺杂氧化铟薄膜在晶硅/非晶硅异质结电池上的应用研究

黄 金[1], 鲍少娟[1], 鲁林峰[2], 杨 骥[1], 白焱辉[1], 张 娟[1], 高 勇[1], 王继磊[1]

(1. 晋能清洁能源科技股份公司 异质结太阳能电池项目研发部，山西 晋中 030300)

(2. 中科院上海高等研究院 薄膜光电中心，上海 201210)

摘 要：采用钛掺杂氧化铟旋转靶制备透明导电薄膜应用在晶硅/非晶硅异质结电池上。在不同氧含量下，研究钛掺杂氧化铟薄膜（T100薄膜）的光电性能，同时对比分析ITO薄膜。在电镜下T100薄膜呈现出柱状结构，并且展示出优异的光学性能。T100薄膜最大载流子迁移率可以达到75.6 cm^2·(V·s)$^{-1}$。相比于ITO薄膜，T100薄膜具有优异的电学传导和透光率，因此在异质结电池量产线上电池转换效率可以实现0.26%的提升。

关键词：钛掺杂氧化铟；透明导电薄膜；异质结电池

作者简介：黄 金，男，1989年生，硕士，晋能清洁能源科技股份公司，山西 晋中 030300，E-mail: 466478431@qq.com